ADVANCING EARTH AND SPACE SCIENCES

JGR Solid Earth

RESEARCH ARTICLE
10.1029/2024JB028805

Magnetic Domain States and Critical Sizes in the Titanomagnetite Series

Brendan Cych[1], Greig A. Paterson[1], Lesleis Nagy[1], Wyn Williams[2], and Bruce Moskowitz[3]

[1]Department of Earth, Ocean and Environmental Sciences, University of Liverpool, Liverpool, UK, [2]School of GeoSciences, Grant Institute, University of Edinburgh, Edinburgh, UK, [3]Department of Earth and Environmental Sciences, Institute for Rock Magnetism, University of Minnesota, Minneapolis, MN, USA

Key Points:

- We systematically map out the domain states in titanomagnetite as a function of shape and composition
- Our results highlight ranges of compositions, shapes and sizes which contain unreliable paleomagnetic recorders
- For certain shapes and compositions, these regions span hundreds of nanometers, representing a significant proportion of remanence carriers

Supporting Information:

Supporting Information may be found in the online version of this article.

Correspondence to:

B. Cych,
bcych@ucsd.edu

Citation:

Cych, B., Paterson, G. A., Nagy, L., Williams, W., & Moskowitz, B. (2024). Magnetic domain states and critical sizes in the titanomagnetite series. *Journal of Geophysical Research: Solid Earth*, *129*, e2024JB028805. https://doi.org/10.1029/2024JB028805

Received 29 JAN 2024
Accepted 4 JUN 2024

Author Contributions:

Conceptualization: Brendan Cych, Greig A. Paterson, Bruce Moskowitz
Data curation: Brendan Cych
Formal analysis: Brendan Cych, Greig A. Paterson
Funding acquisition: Greig A. Paterson, Lesleis Nagy, Wyn Williams
Investigation: Greig A. Paterson, Bruce Moskowitz
Methodology: Brendan Cych, Greig A. Paterson
Project administration: Greig A. Paterson
Resources: Lesleis Nagy, Wyn Williams
Software: Brendan Cych, Lesleis Nagy, Wyn Williams
Supervision: Greig A. Paterson, Wyn Williams

Abstract The minerals carrying the magnetic remanence in geological samples are commonly a solid solution series of iron-titanium spinels known as titanomagnetites. Despite the range of possible compositions within this series, micromagnetic studies that characterize the magnetic domain structures present in these minerals have typically focused on magnetite. No studies systematically comparing the domain-states present in titanomagnetites have been undertaken since the discovery of the single vortex (SV) structure and the advent of modern micromagnetism. The magnetic properties of the titanomagnetite series are known to vary strongly with composition, which may influence the domain states present in these minerals, and therefore the magnetic stability of the samples bearing them. We present results from micromagnetic simulations of titanomagnetite ellipsoids of varying shape and composition to find the size ranges of the single domain (SD) and SV structures. These size ranges overlap, allowing for regions where the SD and SV structures are both available. These regions are of interest as they may lead to magnetic instability and "partial thermal remanent magnetization (pTRM) tails" in paleointensity experiments. We find that although this SD + SV zone occupies a narrow range of sizes for equidimensional magnetite, it is widest for intermediate (TM30-40) titanomagnetite compositions, and increases for both oblate and prolate particles, with some compositions and sizes having an SD + SV zone up to 100s of nm wide. Our results help to explain the prevalence of pTRM tail-like behavior in paleointensity experiments. They also highlight regions of particles with unusual domain states to target for further investigation into the definitive mechanism behind paleointensity failure.

Plain Language Summary Rocks that record Earth's magnetic field often contain the mineral magnetite. The crystal structure of magnetite allows titanium atoms to substitute for iron, giving rise to a range of minerals known as titanomagnetites. The internal magnetic structure of titanomagnetite particles in rocks, known as the "domain structure," controls the ability of that particle to record magnetic fields. Particles with certain kinds of domain structure are unstable magnetic recorders, which can cause problems for experiments trying to determine Earth's magnetic field strength in the past (paleointensity experiments). Although the domain structures in magnetite are well understood, there are no recent studies which describe them in titanomagnetites. In this paper, we simulate the domain structures in small titanomagnetite particles and map these out as a function of size, shape and chemical composition. In doing so, we identify types of magnetic particles with multiple possible domain structures that may give rise to unstable magnetizations. Our results indicate that some titanomagnetite particles may have unstable magnetizations over a much larger range of sizes than has previously been seen in magnetite. This wide range of sizes could explain the high failure rates of paleointensity experiments.

1. Introduction

Magnetite is one of the most important magnetic minerals in igneous and sedimentary rocks, commonly forming during the crystallization of basaltic magmas, and in sediments through erosional and biogenic processes. Stoichiometrically pure magnetite (Fe_3O_4) is a well studied magnetic mineral, but in nature it forms a solid solution series with titanium rich ulvospinel (Fe_2TiO_4). Titanomagnetite compositions within the series $Fe_{3-x}Ti_xO_4$ ($0 \le x \le 1$) are represented using the notation TMx (e.g., $x = 0.6$ is TM60). Fundamental magnetic properties of the titanomagnetites, including the Curie temperature (Nishitani & Kono, 1983), saturation magnetization (Bleil, 1976) and magnetocrystalline anisotropy constants (Kąkol et al., 1994), have been observed to vary across the solid solution series. The distribution of Curie temperatures in igneous rocks

ADVANCING EARTH AND SPACE SCIENCES

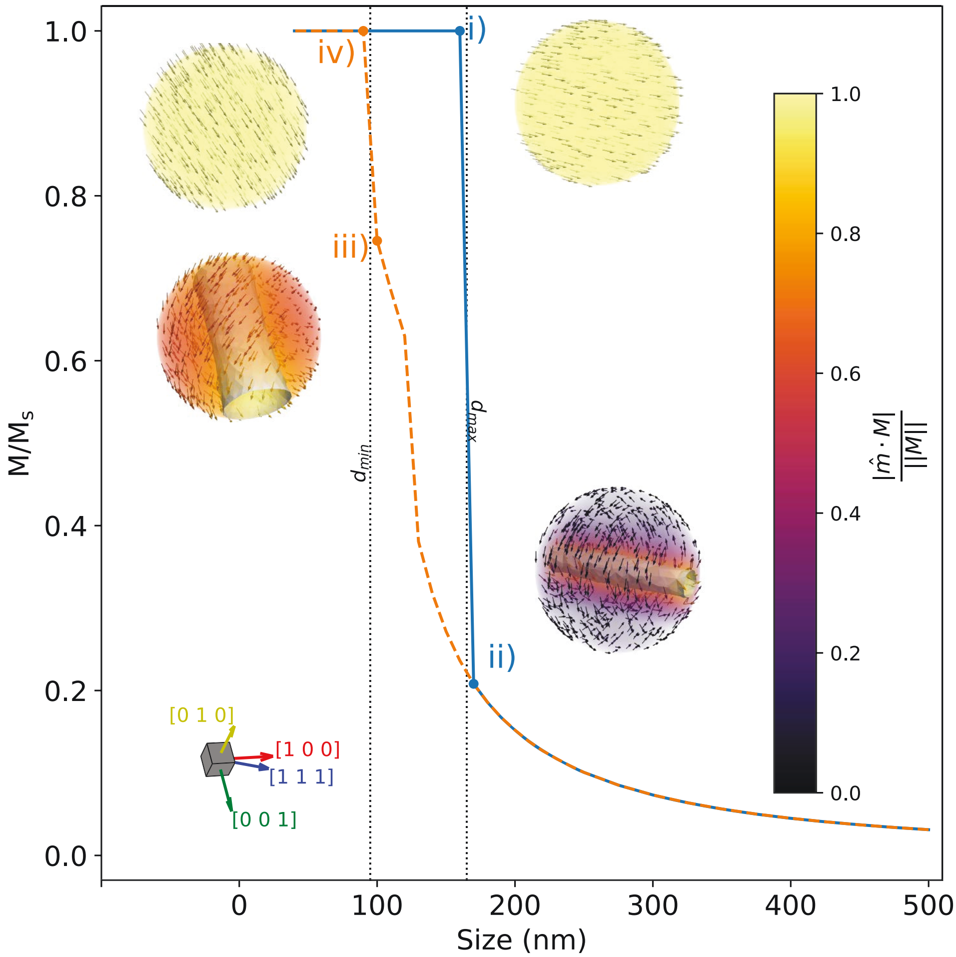

Figure 1. Ratio of the magnetization over the saturation magnetization (M/M_s) plotted against size (nm) in a "size hysteresis loop" for a sphere of TM25. The blue solid line represents the magnetization as the particle is grown from 40 from 500 nm, and the orange dashed line represents the magnetization as it is shrunk from 500 to 40 nm. Example magnetization states from the loop are shown at points (i)–(iv). Vectors represent the direction of the magnetization at that location in the particle. Gray cylinder in (ii) and (iii) represents the "vortex core," an isosurface where the relative helicity (h_{rel}, described in Supporting Information S1) is 0.95. Colors represent the absolute value of the dot product of these vectors with the direction of the net magnetization, with lighter yellow regions being aligned with the net magnetization, and darker purple regions being perpendicular. The cube and vectors in the bottom left of the figure display the orientation of the magnetocrystalline axes in states (i)–(iv). The magnetization transitions from the single domain (SD) to the vortex state between (i) and (ii) (160–170 nm) and the magnitude of the magnetization continues to be reduced up to 500 nm due to the tightening of the vortex core. The vortex rotates to a magnetocrystalline hard axis direction between (ii) and (iii) and transitions back into a SD state between (iii) and (iv) (100–90 nm) along a different easy direction. $d_{\min}$ and $d_{\max}$ are plotted as vertical lines.

increasing the number of particles by more than an order of magnitude. We discuss the implications of these results, as well as the potential impact on paleomagnetic experiments in Section 4.

2. Methodology

2.1. The Size Hysteresis Algorithm

For each geometry and titanomagnetite composition in this paper, we use a "size hysteresis" algorithm. A graphical example for a sphere of TM25 is shown in Figure 1. The algorithm works as follows:

1. For a 40 nm particle of a particular titanomagnetite composition and geometry, start with a uniform magnetization aligned along one of the magnetocrystalline easy axes in zero external field. An energy minimization is performed using MERRILL on this particle, producing a magnetization that is a local energy minimum (LEM) state.

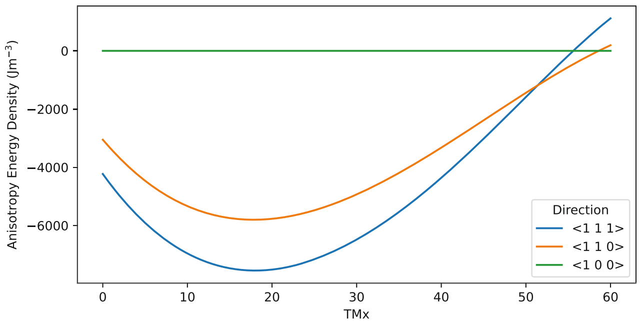

Figure 2. Magnetocrystalline anisotropy energy densities for an single domain titanomagnetite particle as a function of composition. Different colored lines are the anisotropy energy density for different magnetocrystalline directions. The line with the lowest (most negative) magnetocrystalline energy density is the easy axis.

determine $d_{\min}$ and $d_{\max}$, the SV structure was identified by the presence of a coherent cylindrical isosurface at $h_{rel} = 0.95$ containing a "vortex core" intersecting the surface of the particle in two places, and the SD structure was identified by the absence of such a core. Examples of SV structures with vortex cores can be seen in Figure 1 ii and iii. When visualizing LEM states, the volume and magnetization arrows are colored by the absolute cosine of the angle between the individual magnetization vectors and the particle's net magnetization. The lighter colors in the cores of vortex structures demonstrate that the bulk of the magnetization is carried in this core, and that the volume of the core influences the magnitude of the net magnetization.

3. Results

3.1. Anisotropy Energies of the Titanomagnetite Series

Figure 2 shows the magnetocrystalline energy densities in SD titanomagnetites for the <1 0 0>, <1 1 0> and <1 1 1> directions obtained from our fit to experimental data for the k_1 and k_2 anisotropy constants. The magnetocrystalline easy axis for a particle can be determined by the lowest (most negative) energy. Anisotropy properties change significantly across the titanomagnetite series, the easy axis is along <1 1 1> for TM0–50, changing to <1 1 0> at ~TM51 and <1 0 0> at ~TM59. The hard axis is <1 0 0> from TM0–55 and changes to <1 1 1> just above TM55. The difference in anisotropy energy between the easy and hard directions reaches a maximum at ~TM20, and is significantly smaller at high TM compositions (≥TM40).

3.2. Observed States

Examples of typical states observed during the size hysteresis algorithm are shown in Figures 1 and 3. Spherical particles behaved as in Figure 1, with the SD structure changing into an SV structure on the growing branch and back to an SD structure on the shrinking branch, usually rotating to a magnetocrystalline hard direction close to $d_{\min}$ on the shrinking branch (Figure 1 iii). The rotation to a magnetocrystalline hard-aligned vortex was occasionally preceded by a rotation to a magnetocrystalline intermediate axis, particularly in TM55 and TM60 particles. SV states aligned with the magnetocrystalline hard axis were found by Nagy et al. (2017) to have extremely low stability, which may be of interest for paleomagnetists. Oblate particles behaved similarly for both ME-SE and MH-SE aniostropies, nucleating a vortex along the short (shape hard) axis of the particle (Figures 3e and 3f).

Different states were observed in prolate particles depending on elongation direction: In ME-SE particles, a vortex state aligned along the major axis persisted up to the maximum size of 500 nm (Figure 3a ii) and down to $d_{\min}$, without any significant changes to the magnetization structure (Figure 3a iii). By contrast, in MH-SE particles, a secondary sharp drop in the magnetization was observed at sizes above $d_{\max}$, with the SV state along the major axis (Figure 3b iii) transitioning to a state with a curved vortex core which had its ends deflected away from the major axis (Figure 3b iv). These cores were deflected in a variety of directions, forming "Banana" or "S" shapes depending on the whether the two ends of the core were deflected in adjacent or opposing directions. The deflected vortex structures persisted to lower sizes on the shrinking branch than on the growing branch, leading to another "loop" on the size hysteresis diagrams. The transition at $d_{\min}$ for MH-SE particles was often more subtle than for ME-SE ones, with little change in energy, and often a closed loop ($d_{\min} = d_{\max}$) for example, Figure 3b i and ii.

The "S" shaped vortices were frequently observed undergoing rotations during the shrinking branch of the size hysteresis loop, with the core rotating to lie along one of the short (shape-hard) axes of the particle, similar to the states observed in Nagy et al. (2022), which were found to cause pTRM tails in paleointensity experiments. This behavior can be seen in Figure 3d i–iv, and occurred most frequently in prolate particles with axial ratios between 1 and 2. This rotation to a short axis was occasionally observed in ME-SE particles, but was far less prevalent overall.

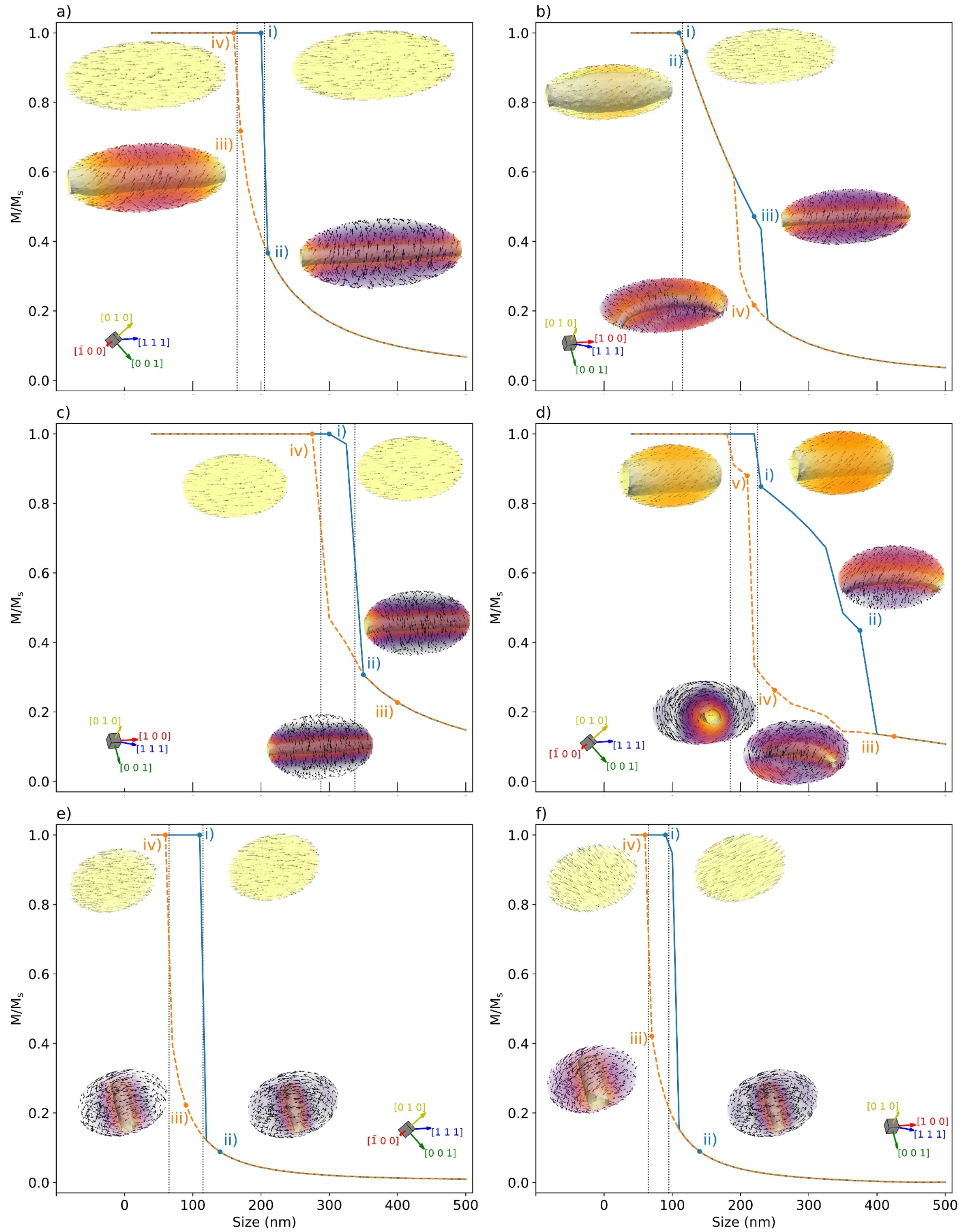
a)
b)
c)
d)
e)
f)
M/Ms
Size (nm)
1.0
0.8
0.6
0.4
0.2
0.0
0
100
200
300
400
500
i)
ii)
iii)
iv)
v)
[0 1 0]
[1 0 0]
[1̄ 0 0]
[1 1 1]
[0 0 1]

. ,) 8 , - /
, - / - /) , C4 - /
' 94) , ? % ,) - /
) , 4 C - / - / - / - / - /)
)) - / - / , (, - /S- /
- / - /

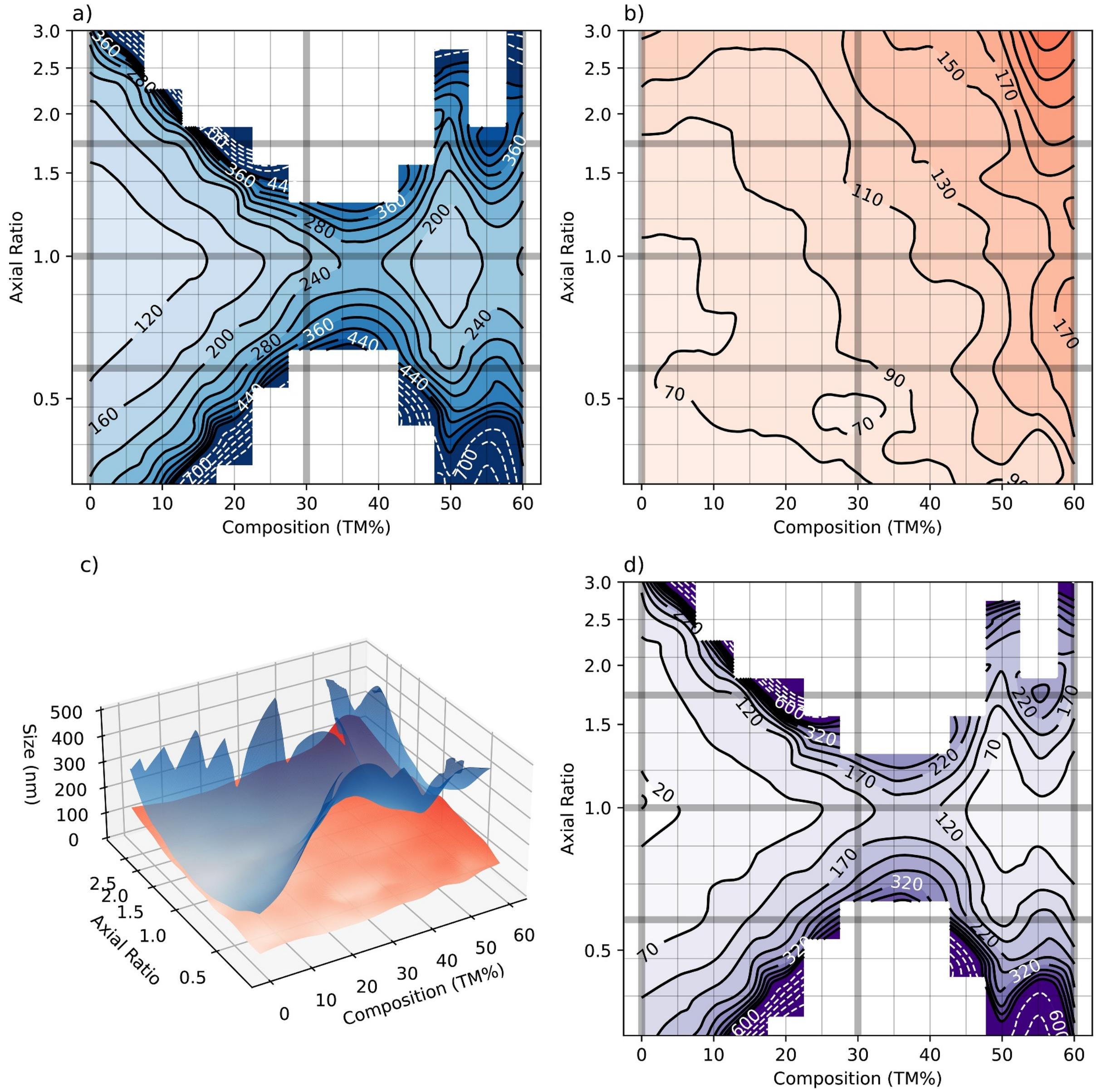

. 7 , , ((
- / : ,) - /)) - / - / :
) , - . /)) - / - / , - / - / - / :
- /)) - /S- / ') .
'))
')) 8 C 0)
44) C44 , 444) %) - / C44 ,
) N

'
,
8 5 ' , ' ,
,)) 0)
44) ,) C44)
& , '

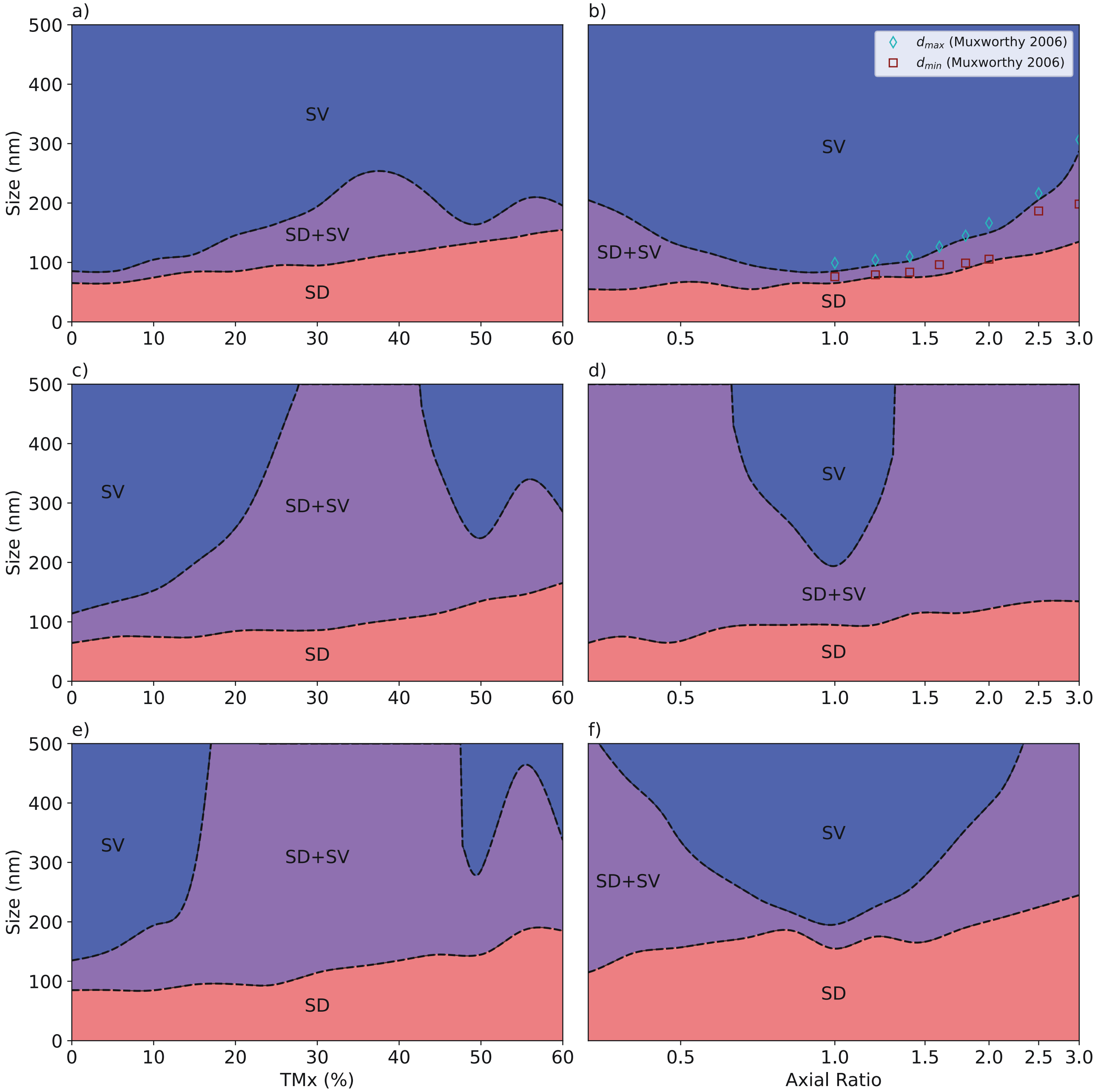

Figure 5. Slices through surfaces displayed in Figure 4. Slices in the left column have constant axial ratio, and slices through the right column have constant composition, with the following values: (a) Axial ratio of 1, (b) TM0 (magnetite), (c) axial ratio of 0.58 (oblate), (d) TM30, (e) axial ratio of 1.73 (prolate), (f) TM60. Blue represents regions above the upper surface where the single vortex (SV) structure (and other more complicated states) is available. Red represents the region in which the single domain (SD) structure is available. Purple represents the range of sizes in which the SD and SV structures are both available. The minimum d_{min} and maximum d_{max} of Muxworthy and Williams (2006) are plotted in (b) as red squares and blue diamonds for comparison with our magnetite data.

state persists beyond 1 μm during the growing branch of the size hysteresis loop. Obtaining d_{min} and d_{max} for loops above this size becomes rapidly more computationally expensive.

The surfaces displayed in Figure 4 exhibit some consistent trends with both size and shape. Slices through these surfaces (represented by thick lines on Figures 4a, 4b, and 4d) at constant composition or axial ratio are displayed in Figure 5. The most noticeable feature of the surfaces is that d_{max} sharply increases for both prolate and oblate particles relative to equidimensional ones for all compositions (Figures 4a and 4c). By contrast d_{min} tends to increase with increasing axial ratio across almost all shapes. The relationship between d_{max} and TM composition

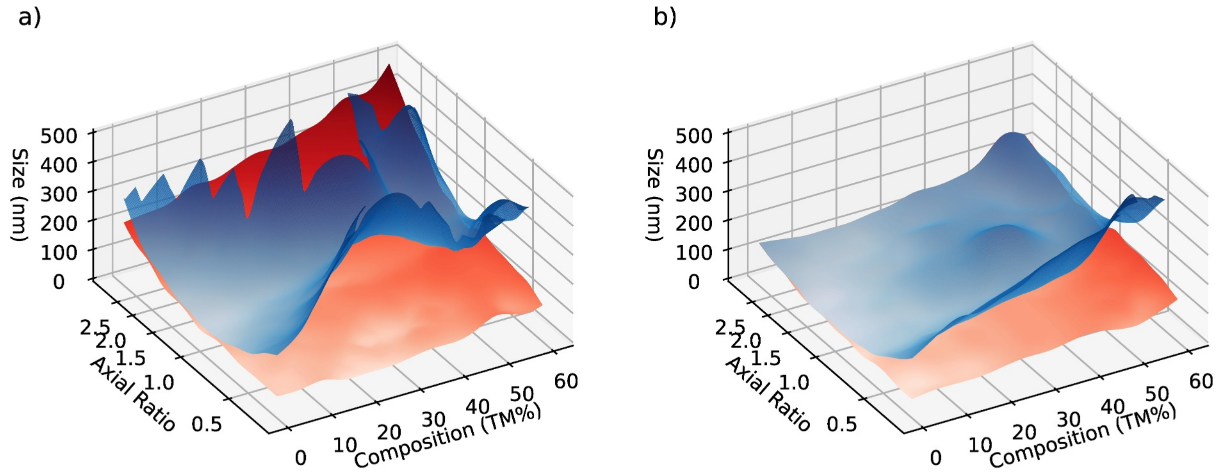

. : : (- / (- / '
8 5

8 3 , ' 4S
' 54 ' 54S' C4) ' CC ' 94 '
))
'

' I (8 9
, 8 5 (, ' '
I ( ) -
/ ' I (,
' (,
-8 / I (
. -8 /) .
) , ' , I (
-8 / '

, 6

K
.))
M - ?C/ (')
) (&
)
M '
)
')
,
' 3 ,) 0 K
- 449/) (0 ,
- . / 8 C ' ,))
' ,) ;
0 , C) '
) (